Deglacial Pulse of Neutralized Carbon from the Pacific Seafloor: Constraints from the Radiocarbon Budget

R. A. Green[1], M. P. Hain[1], and P. A. Rafter[2]

[1] Earth and Planetary Science Department, University of Santa Cruz, Santa Cruz, USA

[2] Department of Earth System Science, University of California, Irvine, CA, USA

Corresponding author: Ryan A. Green (rygreen@ucsc.edu)

Key Points:

- Observed deglacial changes in atmospheric CO_2 and $^{14}C/C$ allow for up to 2397 Pg of neutralized geologic carbon (i.e., bicarbonate) release
- Inverse modeling yields two bicarbonate pulses that are insufficient to drive basin-scale ^{14}C anomalies and have limited CO_2 effect
- The global carbon cycle is essentially "blind" to neutralized carbon release and only constrained by ^{14}C budget

Abstract

In the intermediate depth Eastern Tropical Pacific Ocean, multiple deglacial radiocarbon (^{14}C) records show anomalously low $^{14}C/C$ values that appear to be best explained by the addition of ^{14}C-free geologic carbon. We use inverse carbon cycle modeling and data assimilation of reconstructed atmospheric CO_2 and $\Delta^{14}C$ to develop an upper bound constraint on this speculated deglacial geologic carbon release. Our analysis suggests two primary opportunities where large bicarbonate pulses (up to 1.3 PgC yr^{-1}) could occur with little effect on atmospheric CO_2 and without upsetting ^{14}C mass-balance constraints. Including the release of ^{14}C-free permafrost carbon and regrowth of the terrestrial biosphere, we obtain a set of permissible scenarios for ocean geologic carbon release that ranges from 900-2400 PgC. Based on these results, we conclude that geologic carbon release is a plausible interpretation for the spatio-temporal cluster of anomalous ^{14}C data near the East Pacific Rise.

Plain language summary

Oceanic records indicate that the Eastern Pacific Ocean contained pockets of extremely old water after the last ice age. The cause of this phenomenon has been puzzling because the water is too old to have been caused by a slowdown of ocean circulation. It was proposed that the old water may have instead been caused by geologic carbon addition since the records are located near volcanically active spreading centers on the seafloor. However, the scale of possible geologic carbon addition is unclear. To help constrain this, we modeled different geologic carbon release scenarios and compared the results with observed atmospheric and ocean data. Our findings indicate that if the geologic carbon were neutralized with equal amounts of alkalinity, then large quantities (up to 6% of the total carbon inventory) could be added to the ocean without causing significant changes to the atmosphere or surrounding ocean regions. Based on these findings, it is possible that large-scale neutralized carbon release occurred since the last ice age and may explain the exceptionally old water in the Eastern North Pacific. This neutralized carbon would unlikely cause significant changes to the atmosphere or greater ocean regions.

1 Introduction

Due to the tight coupling of the carbon cycle and climate (Marcott et al., 2014), we must understand how the natural carbon cycle has changed in the past. An unexplained feature of the natural carbon cycle is the presence of anomalously low radiocarbon ($^{14}C/C$) content–relative to the contemporaneous atmosphere and most parts of the global ocean–within marine foraminifera between 18,000 and 11,500 years before 1950 (18-11.5 thousand years before present or kyr BP, Fig. 1). These deglacial records of ^{14}C depletion (decay-corrected ^{14}C:^{12}C ratio, expressed as $\Delta^{14}C$; Stuiver & Polach, 1977) have been uncovered throughout the intermediate-depth (<1000m) Pacific Ocean (Lindsay et al., 2016; Marchitto et al., 2007; Rafter et al., 2018, 2019; Stott et al., 2009). Occurring roughly at the same time as the deglacial rise in atmospheric CO_2 and near the weakly ventilated Pacific shadow zone (Gehrie et al., 2006; Holzer et al., 2021), these depletions in seawater $\Delta^{14}C$ were initially attributed to a release of dissolved inorganic carbon (DIC) that had been sequestered for thousands of years in the abyssal ocean, hinting at deglacial changes in ocean circulation (Bova et al., 2018; Broecker, 2009; Broecker & Barker, 2007; Marchitto et al., 2007). However, this ocean release interpretation has two main shortcomings (Hain et al., 2011): (a) the LGM deep ocean was not sufficiently ^{14}C-depleted (Fig. 1) to be the source of the mid-depth anomalies, and (b) once the isotopic signature of anomalously ^{14}C-depleted carbon is transported to the mid-depth Pacific it would rapidly dissipate into the global carbon cycle via ocean circulation and air/sea gas exchange. This view is further supported by a new compilation showing no appreciable ^{14}C-depletion at any depth for the basin-scale Pacific during the deglaciation (Fig. 1; Rafter et al., 2022). Additionally, deep-sea coral ^{14}C records from the Galápagos with excellent age model controls (Fig. 1; Chen et al., 2020) and South Pacific ^{14}C records bathed in modern Antarctic Intermediate Water (De Pol-Holz et al., 2010; Rose et al., 2010; Siani et al., 2013; Zhao & Keigwin, 2018) show no significant ^{14}C-depletion. This lack of basin-wide mid-depth $\Delta^{14}C$ depletion is an important observational constraint we will consider below.

An alternative set of proposals suggest these anomalously low $\Delta^{14}C$ values reflect an addition of ^{14}C-free carbon from a geologic source (Rafter et al., 2018, 2019; Ronge et al., 2016; Skinner & Bard, 2022; Stott et al., 2009; Stott & Timmermann, 2011). A common objection to this hypothesis is the potential for ocean acidification, which would contradict the evidence supporting enhanced carbonate preservation during the last deglacial (Allen et al., 2015, 2020; Cartapanis et al., 2018; Marchitto et al., 2005; Yu et al., 2013). However, if the geologic carbon addition was neutralized by a commensurate influx of alkalinity (e.g., carbon added as bicarbonate ion instead of CO_2)—there would be muted effects on seawater pH, $CaCO_3$ burial, and atmospheric CO_2 (Rafter et al., 2019).

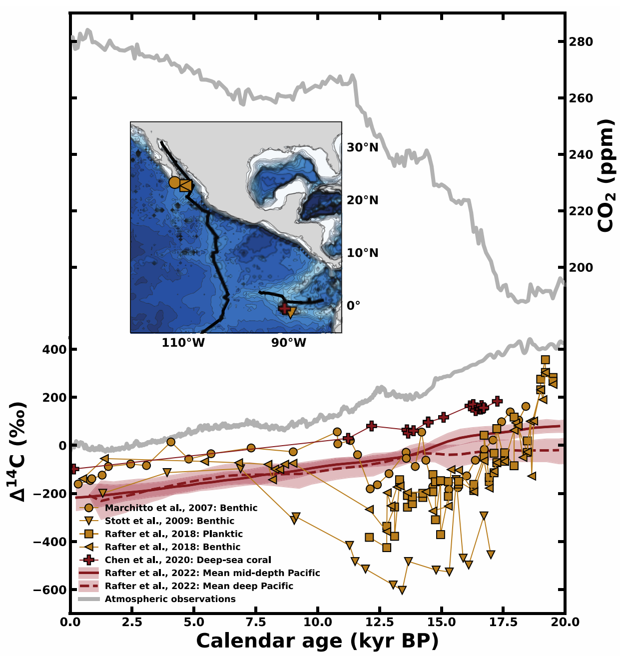

Figure 1. Deglacial intermediate-depth (< 1000m) $\Delta^{14}C$ records (red and yellow) compared to atmospheric $\Delta^{14}C$ and CO_2 (gray). *Yellow records (foraminifera) show anomalously low $\Delta^{14}C$ values, while red records (foraminifera and coral) broadly track atmospheric $\Delta^{14}C$. The solid red line shows the mean mid-depth $\Delta^{14}C$, and the dashed red line shows the mean deep Pacific $\Delta^{14}C$ for all Pacific sites from Rafter et al. (2022). The red shading indicates the 95% confidence interval error envelope. Locations of individual $\Delta^{14}C$ records are shown in the map, with ocean bathymetry and the East Pacific Rise spreading center (black lines).*

This neutralized ^{14}C-free carbon–likely produced within marine sediments (Rafter et al., 2019; Skinner & Bard, 2022)–would eventually be transported to the upper water column and atmosphere, diluting the atmospheric ^{14}C reservoir and lowering atmospheric $\Delta^{14}C$. Although there was a rapid decline in atmospheric $\Delta^{14}C$ during the last deglaciation, also known as the 'mystery interval' (Broecker, 2009; Broecker & Barker, 2007), this $\Delta^{14}C$ decline can mostly be explained by Southern Ocean CO_2 release, Atlantic circulation changes, and the cosmogenic decline in ^{14}C production (Hain et al., 2014), leaving limited opportunities in the planetary ^{14}C budget for the addition of ^{14}C-free geologic carbon.

Moreover, terrestrial carbon cycle changes, such as permafrost destabilization (release of ^{14}C-depleted CO_2) and regrowth of the land biosphere (uptake of ^{14}C-enriched CO_2), are thought to have occurred during the last deglaciation (Adams et al., 1990; Behling, 2002; Ciais et al., 2012; Crichton et al., 2016; Köhler et al., 2014; Lindgren et al., 2018), and would further influence the opportunity for ^{14}C-free geologic carbon addition. With multiple established mechanisms lowering deglacial atmospheric $\Delta^{14}C$, is there room in the ^{14}C budget for geologic carbon release?

In this study, we incorporate these terrestrial processes alongside submarine geologic carbon release into the deglacial model scenario from Hain et al. (2014) to simulate their combined effect on atmospheric CO_2 and the planetary ^{14}C budget. We use a stepwise numerical model optimization method that assimilates observed atmospheric CO_2 and $\Delta^{14}C$ data into the model to find the optimal rate of geologic carbon and alkalinity release. This optimization yields an upper bound limit on the amount of geologic carbon that could have been added since the LGM and characterizes the chemical speciation (i.e., CO_2, HCO_3^-, or CO_3^{2-}) of that geologic carbon release. These results provide valuable insight into the sensitivity of the global carbon cycle after various open-system carbon perturbations, ultimately allowing us to show that geologic carbon addition remains a viable explanation for the deglacial $\Delta^{14}C$ anomalies.

2 Materials and Methods

We use the CYCLOPS global carbon cycle model (Hain et al., 2010, 2011, 2014; Keir, 1988; model configuration described in supplementary material) to simulate four experiments, progressively adding optimized and imposed open-system carbon and alkalinity fluxes (Fig. 2): (1) we invert for the optimal rates of carbon and alkalinity release to the mid-depth North Pacific region of the model (experiment NP), (2) we add the possibility of land carbon uptake to the optimization (experiment NP+LC), (3) we include the release of ^{14}C-free permafrost carbon (experiment NP+LC+PF), and (4) we adjust the initial LGM ^{14}C inventory by +3.5% (experiment NP+LC+PF+RC). All experiments include the identical background forcings of the control run, based on the deglacial carbon cycle scenario from Hain et al. (2014). More in-depth descriptions of the experiments can be found in the supplementary material (SM). The optimized fluxes are determined by a numerical algorithm that minimizes the deviation between simulated atmospheric CO_2 (CO_2^{model}) and $\Delta^{14}C$ ($\Delta^{14}C^{model}$) compared to reconstructed atmospheric CO_2 (CO_2^{obs}) from the most recent compilation of Antarctic ice core CO_2 data (Bereiter et al., 2015) and $\Delta^{14}C$ ($\Delta^{14}C^{obs}$) from IntCal20 (Reimer et al., 2020)**.** Details of the algorithm can be found in the SM.

3 Results

3.1 Atmospheric constraints on geologic carbon addition

All four simulations improve the overall CO_2 and $\Delta^{14}C$ model-data misfit compared to the control run (blue vs. black line, Fig. 2). This model-data misfit is progressively minimized as more open-system carbon and alkalinity fluxes are added to the model, with the NP+LC+PF+RC simulating the smallest model-data misfit. Each simulation has two main pulses of geologic carbon during the deglaciation and one smaller pulse during the Holocene. These geologic pulses occur when $\Delta^{14}C^{model}$ rises above $\Delta^{14}C^{obs}$, which we call ^{14}C opportunities. Majority of the geologic carbon is added as bicarbonate ion (61-84%, Table S1), with net ALK-to-DIC ratios between 1.08 and 1.19 (Table S1) across all four simulations. We note there is a small carbonate ion pulse that occurs only during the Holocene of the NP simulation (Fig. 2i). The algorithm adds carbonate to counteract a CO_2 misfit of ~20 ppm during the Holocene (Fig. 2e) that emerged due to simulated alkalinity loss from ongoing carbonate compensation (raising atmospheric CO_2) in conjunction with the underlying CO_2 rise from Holocene Southern Ocean changes found in our control run (Hain et al., 2014). Only the NP simulation simulates this carbonate pulse because the other models include terrestrial regrowth, thus minimizing the Holocene CO_2 misfit with land carbon uptake instead (Fig. 2j-l).

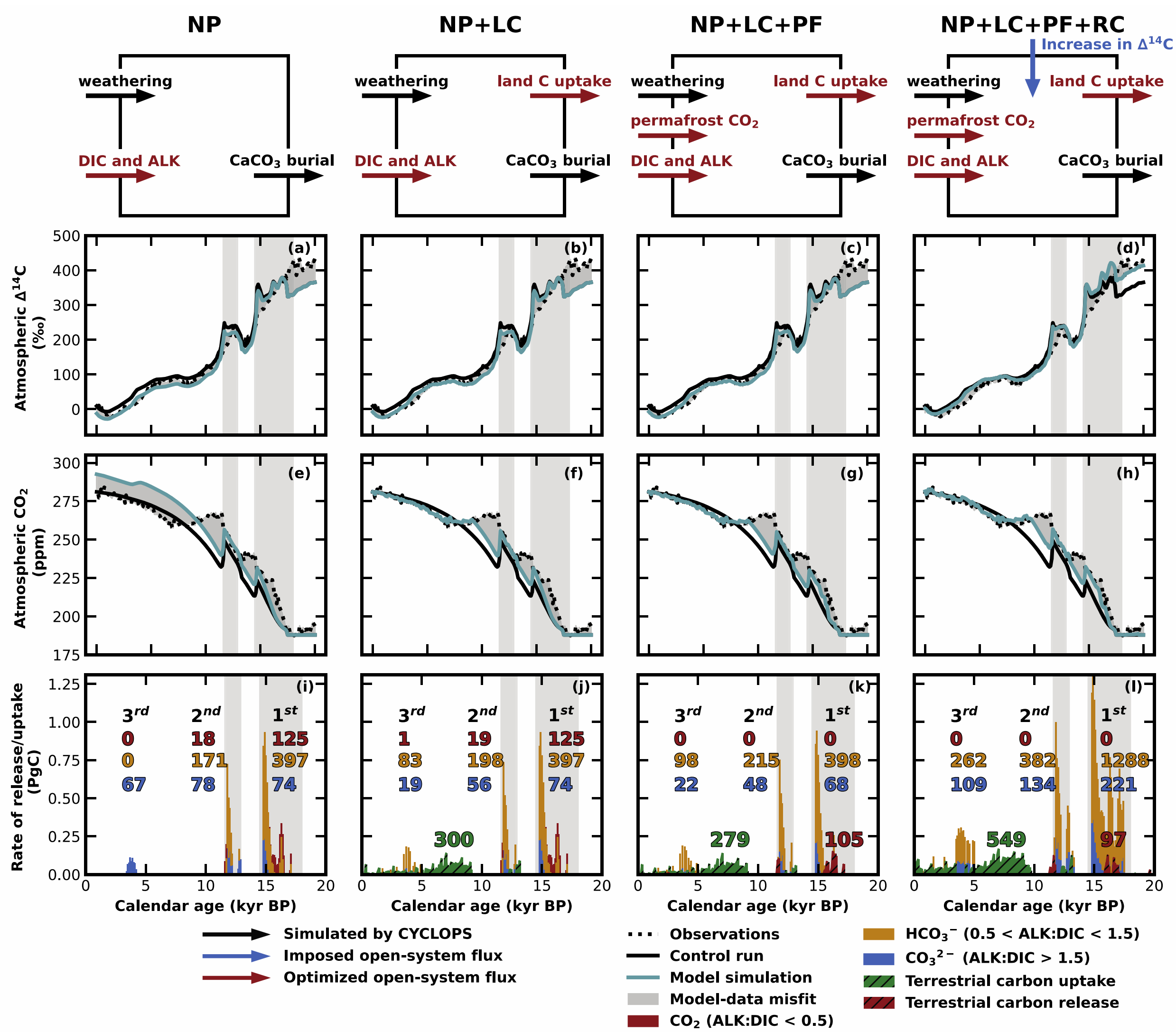

Figure 2. Visual representation of each experiment and the simulation results . *Cartoons in the top row show the progressive addition of optimized and imposed open-system fluxes (colored arrows) for each experimental simulation. The other rows show atmospheric $\Delta^{14}C$ (a-d), atmospheric CO_2 (e-h), and the rate of carbon release or uptake (i-l). In panels i-l, the colored numbers show the amount of CO_2 (red), HCO_3^- (yellow), and CO_3^{2-} (blue) for each pulse of geologic carbon release. Similarly, the amount of terrestrial carbon uptake is shown in green,*

and the amount of terrestrial carbon release is shown in red. All colored numbers are in units of PgC.

For our first three experiments (NP, NP+LC, NP+LC+PF)–which include no change to the ^{14}C inventory–geologic carbon was added at rates as large as 0.93 PgC yr^{-1} (Fig 2i-k), totaling between 846-929 PgC over the 20-kyr experiment (Table S1). Of those that included terrestrial regrowth (NP+LC, NP+LC+PF), between 279-300 PgC (Table S1) of simulated carbon uptake occurs, mainly during the Holocene. When we include terrestrial carbon release from permafrost thaw (NP+LC+PF), 105 PgC (Fig 2k, Table S1) is released around 16-kyr BP and during the first pulse of carbon addition. Our fourth experiment, NP+LC+PF+RC, includes an adjusted ^{14}C inventory at the LGM initial state alongside all the above open-system fluxes. The higher initial model $\Delta^{14}C$ increases the opportunity for the subsequent addition of ^{14}C-free carbon, leading to higher rates of carbon addition (up to 1.3 PgC yr^{-1}, Fig. 2l) and a greater amount of total carbon added (2396 PgC, Table S1). Consequently, land carbon uptake increases to 550 PgC (Table S1). NP+LC+PF+RC simulates the release of 97 PgC from permafrost thaw around 16-kyr BP.

3.2 Additional constraints on geologic carbon addition

We also consider local effects–regional $\Delta^{14}C$, $CaCO_3$ burial, and regional $\delta^{13}C$–to further constrain the geologic carbon release hypothesis. For NP+LC+PF+RC (the largest geologic carbon addition scenario), only minor $\Delta^{14}C$ anomalies are simulated in the intermediate depth North Pacific box where the carbon is released (solid turquoise line, Fig. 3a). The $\Delta^{14}C$ deviation from the control run (dotted turquoise line, Fig. 3a) is shown with turquoise shading (Fig. 3a). Although NP+LC+PF+RC is our most extreme geologic carbon addition simulation, the simulated intermediate depth North Pacific $\Delta^{14}C$ (solid turquoise line) is in broad agreement with the mean $\Delta^{14}C$ from the mid-depth (neutral density of 27.5–28 kg m^{-3}) Pacific, calculated from a new proxy $^{14}C/C$ compilation (red line-Fig. 3a, Rafter et al., 2022). Furthermore, the lack of severe $\Delta^{14}C$ depletion found in the NP+LC+PF+RC simulation is supported by a deep-sea coral record considered representative of the ^{14}C content of intermediate waters near the Galápagos islands (Chen et al., 2020).

Figure 3b shows the Atlantic (blue) and Indo-Pacific (yellow) deep ocean $[CO_3^{2-}]$ from the NP+LC+PF+RC and control simulation. An increase in deep-ocean $[CO_3^{2-}]$ would promote the preservation and burial of $CaCO_3$ in sediments. Both simulations show two transient increases in $[CO_3^{2-}]$, during and after HS1 and YD in the Indo-Pacific and in the Atlantic (gray shaded areas, Fig. 3b), as well as simulating an overall increase in Atlantic $[CO_3^{2-}]$ from the LGM to the Holocene. After 1509 PgC is added during the first pulse (Skinner & Bard, 2022)e of geologic carbon addition (Fig. 2l), NP+LC+PF+RC simulates a ~10 µmol kg^{-1} in Atlantic $[CO_3^{2-}]$ and a ~5 µmol kg^{-1} increase in Indo-Pacific CO_3^{2-} for the remainder of the simulation compared to the control run (shaded blue and yellow). The simulated increase in Atlantic $[CO_3^{2-}]$ since the LGM and the transient increase in the Indo-Pacific [CO_3^{2-}] between 11 and 15-kyr BP is supported by the observations shown in Figure 3b (Yu et al., 2008, 2010).

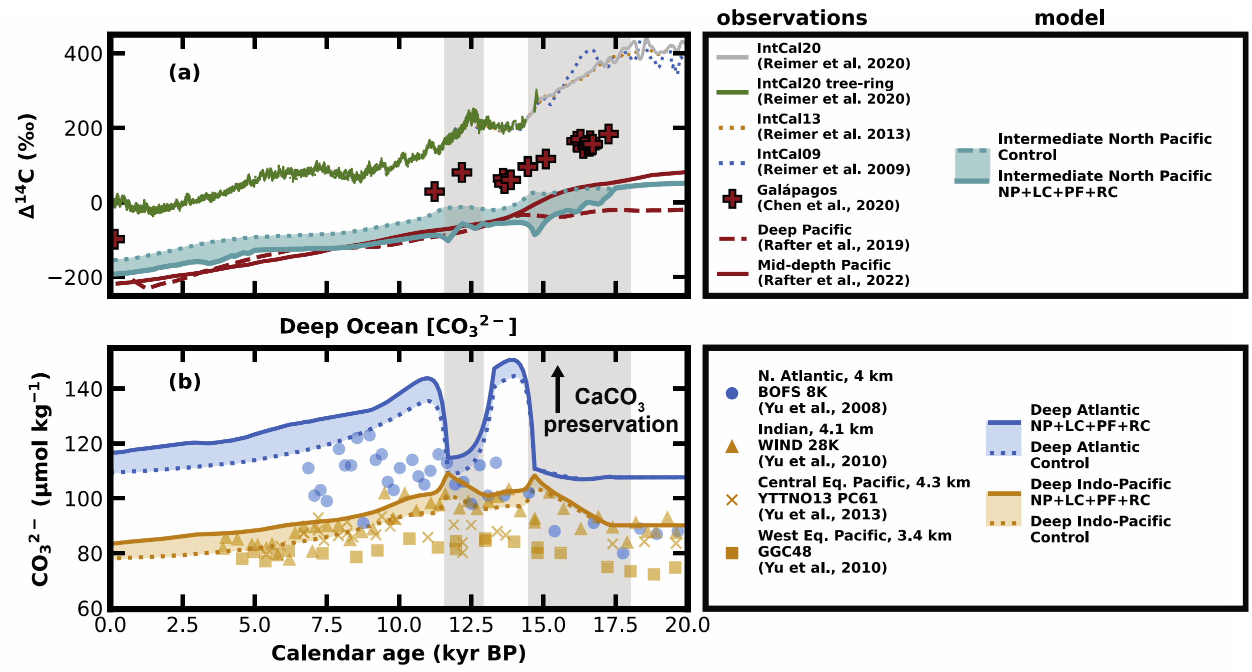

Figure 3. Comparing the NP+LC+PF+RC simulation to observations. *Panel a shows NP+LC+PF+RC driving only mild Δ^{14}C depletion from the control run (shaded turquoise area), in broad agreement with other datasets that show no noticeable Δ^{14}C depletion, i.e., Δ^{14}C from deep-sea coral near the Galápagos (red plus sign), the mean Δ^{14}C from mid-depth and deep Pacific (solid and dashed red line), and atmospheric Δ^{14}C (solid gray and green, dotted yellow and blue). We note the atmospheric Δ^{14}C disagreement near the LGM across the last three iterations of IntCal, before converging as tree-ring data becomes available (solid green line). Panel b shows NP+LC+PF+RC driving an increase [CO_3^{2-}], indicative of a $CaCO_3$ preservation event, in the Atlantic (blue) and Indo-Pacific deep ocean basins (yellow) compared to the control run (shaded blue and yellow). These simulated deep ocean [CO_3^{2-}] are in broad agreement with observations from the North Atlantic (blue circle), Indian (yellow triangle), and Equatorial Pacific (yellow square and X). The gray bars show Heinrich Stadial 1 and Younger Dryas.*

We have focused on Δ^{14}C rather than δ^{13}C for two reasons. First, Δ^{14}C is corrected for mass and temperature-dependent isotopic fractionation (Stuiver & Polach, 1977). Thus, isotopic gradients in the Δ^{14}C record can be attributed directly to changes in production, transport, and/or decay of ^{14}C. Second, we know the Δ^{14}C of geologic carbon (^{14}C-free) but not the δ^{13}C value, which varies depending on the geologic source. To constrain which geologic sources are plausible, we run an additional set of experiments by calculating the bulk ocean δ^{13}C change for two possible neutralized geologic sources (described in SM): bicarbonate from anaerobic oxidation of thermogenic methane (AOM, see Rafter et al. 2019; δ^{13}C = -25‰), and geologic CO_2 neutralized by carbonate dissolution (Skinner & Bard, 2022; δ^{13}C = -2.5‰). While δ^{13}C values could vary within the range of -25 to -2.5‰, the test cases utilized in this study are treated as endmember scenarios. When 2400 PgC (as suggested by our NP+LC+PF+RC experiment) is added, we observe bulk $\delta^{13}C$ ocean changes of -1.5‰ for AOM and -0.2‰ for carbonate dissolution. Given that observed oceanic $\delta^{13}C$ values have not fluctuated more than ~1‰ over the last 800-kyrs (Hodell et al., 2003), our simulations suggest geologic carbon from a methane source ($\delta^{13}C$ <= -25‰) is unlikely for our extreme carbon addition scenario of 2400 PgC.

4 Discussion

Our results indicate that the atmospheric CO_2 and $CaCO_3$ burial constraints are effectively blind to carbon release neutralized by alkalinity (i.e., carbon added as bicarbonate, HCO_3^-). This allows for large-scale geologic carbon addition scenarios constrained by only the planetary radiocarbon budget. Additionally, these large-scale carbon addition scenarios did not drive significant $\Delta^{14}C$ depletion across the North Pacific, in agreement with observations representative of the North Pacific and Pacific basins. This supports the idea that these enigmatic $\Delta^{14}C$ anomalies are likely regional or localized phenomena that may still be explained by geologic carbon addition.

4.1 Large amounts of bicarbonate allowable

We optimized our carbon cycle modeling simulations, which include different open-system fluxes and changes to the ^{14}C inventory, with the addition of geologic carbon. The simulations show that up to 2397 Pg of geologic carbon, mainly as bicarbonate ion, can be consistent with the observed deglacial changes in atmospheric CO_2 and $\Delta^{14}C$. Due to the alkalinity accompanying DIC during bicarbonate addition, geologic carbon in this form can be added at rates as large as 1.3 PgC yr^{-1} (Fig. 2l) with limited impacts on atmospheric CO_2 and deep-sea [CO_3^{2-}].

Prior work has estimated that deglacial geologic CO_2 emissions from mantle decompression could have reached up to 0.2 PgC yr^{-1} (Cartapanis et al., 2018; Roth & Joos, 2012), much smaller than our maximum yearly rates. However, these lower rates were derived assuming the geologic carbon came only as CO_2 rather than as bicarbonate ion. When carbon is added without alkalinity (i.e., CO_2), atmospheric CO_2 and $CaCO_3$ burial constraints are highly sensitive to any carbon added to the system. However, when adding neutralized carbon (bicarbonate), atmospheric CO_2 and $CaCO_3$ burial constraints become effectively blind to the carbon release, no longer constraining the carbon release rate or total. During bicarbonate addition, the constraining factor shifts to the planetary ^{14}C mass balance and its reflection in the atmospheric $\Delta^{14}C$ record (via IntCal20, Reimer et al., 2020), which can indirectly record the dilution of ^{14}C-enriched environmental carbon by ^{14}C-free geologic carbon. This $\Delta^{14}C^{obs}$ constraint on bicarbonate release leads to an upper bound of 800-1000 PgC in all our open-system simulations (NP, NP+LC, NP+LC+PF)—a 2-2.5% increase of total ocean carbon inventory. Furthermore, if we take into consideration the uncertainty in the planetary ^{14}C mass balance (Dinauer et al., 2020; Roth & Joos, 2013) by increasing the initial LGM ^{14}C inventory by 3.5%, the opportunity for subsequent geologic carbon release increases to ~2500 PgC (6.5% increase of total ocean carbon inventory). In other words, a higher initial LGM $^{14}C/C$ can substantially increase the opportunity for ^{14}C-free geologic carbon release since the LGM.

Considering the idealized nature of our experiments and because of biases inherited from our control run (Hain et al., 2014), our optimization results should not be taken as estimates of geologic carbon release or of other simulated open-system carbon fluxes (e.g., LC, PF). Instead, we argue that geologic carbon release greater than 800 -1000 PgC is rendered unlikely, and release of greater than 2400 PgC is implausible in the face of the $\Delta^{14}C^{obs}$. Further, if indeed there was substantial geologic carbon release since the LGM, it must have been in the neutralized form of bicarbonate ion with a net ALK-to-DIC ratio near 1, as proposed by Rafter et al. (2019), to avoid violating constraints from atmospheric CO_2 and $CaCO_3$ burial. Therefore, we argue that geologic carbon release played only a minor role in raising CO_2 at the end of the last ice age, even if the total amount of carbon release was substantial. This contrasts with prior deglacial geologic carbon addition research, which attributes glacial/interglacial CO_2 variability to liquid CO_2 release (Stott et al., 2019; Stott & Timmermann, 2011).

4.2 Geologic carbon as an explanation for $\Delta^{14}C$ anomalies?

When first discovered, the $\Delta^{14}C$ anomalies in the ETNP were taken to be the signature of carbon release from the deep ocean to the atmosphere (Marchitto et al., 2007). This earlier view of the $\Delta^{14}C$ anomalies buttresses the longstanding notion that stagnation of deep ocean circulation during the LGM created an isolated ^{14}C-deplete reservoir for the sequestration of atmospheric CO_2 (Broecker & Barker, 2007; Skinner et al., 2010)—and this view remains prevalent (e.g., Bova et al., 2018). However, deep ocean carbon storage and its effect on atmospheric CO_2 is more closely tied to the degree of nutrient consumption in the polar ocean regions that form new deep water (Hain et al., 2010, 2014; Ito & Follows, 2005; Marinov et al., 2008a, 2008b; Sigman et al., 2010, 2021; Sigman & Haug, 2003) rather than being a simple function of the rate of deep ocean overturning. Further, a new compilation of global ocean $\Delta^{14}C$ records reveals that the LGM ^{14}C age of the global deep ocean was about ~1000 years greater than today (Rafter et al., 2022), sufficient to explain a large portion of the observed $\Delta^{14}C^{obs}$ decline during the deglacial period (Broecker & Barker, 2007; Hain et al., 2014), but not nearly ^{14}C-deplete enough to produce the ETNP $\Delta^{14}C$ anomalies (Fig. 3a). Rather than becoming a plank in our evolving understanding of coupled glacial/interglacial changes in ocean circulation and the global carbon cycle, the existence of these $\Delta^{14}C$ anomalies has become its own vexing problem, defying conventional explanations based on ocean circulation.

There are numerous reasons why a given sample would yield an anomalously low reconstructed $^{14}C/C$, but the spatial-temporal clustering of ^{14}C anomalies in the upper 1 km of the ETNP water column is remarkable (e.g., Bova et al., 2018; Lindsay et al., 2015; Marchitto et al., 2007; Rafter et al., 2018, 2019; Stott et al., 2019), especially when contrasted with nearby records that broadly track atmospheric ^{14}C change without discernible ^{14}C anomalies (e.g., Bova et al., 2018; Chen et al., 2020; De Pol-Holz et al., 2010; Rose et al., 2010; Siani et al., 2013; Zhao & Keigwin, 2018). Previous modeling of the problem suggests that any ^{14}C anomaly in the upper ocean would rapidly dissipate by ocean circulation and air/sea gas exchange (Hain et al., 2011) such that upper ocean $\Delta^{14}C$ is expected to track atmospheric $\Delta^{14}C$ change since the LGM (Hain et al., 2014), as is observed in independently dated coral ^{14}C records from the Atlantic and Pacific (e.g., Chen et al., 2020) and other records outside the anomalous ETNP cluster. Our new results advance the argument by demonstrating that even the release of >2000 PgC is insufficient to generate a significant ^{14}C anomaly on the basin scale resolved in the model (Fig. 3a). That is, the absence of anomalies in most upper ocean ^{14}C reconstructions are normal and expected even in the case of substantial simulated carbon release. The caveat to the argument is that a small $\Delta^{14}C$

reduction simulated at the basin scale would be consistent with a severe ^{14}C anomaly concentrated in a small sub-region, such as observed in the ETNP.

If not continuously sourced from a persistently ^{14}C-depleted upstream water mass signature (e.g., Hain et al., 2011), the ^{14}C anomalies of the ETNP may instead record carbon release associated with processes linked to spreading centers separating the Cocos, Nazca, and Pacific plates and the very high regional geothermal heat flux (>0.1 W m^{-2} throughout the region; Pollack et al., 1993). While we cannot usefully comment on whether these geologic systems are dynamic enough to yield defined pulses of carbon release, our results highlight that only a neutralized form of carbon release would be consistent with the atmospheric CO_2 constraint and observations of good (sometimes improved) seafloor carbonate preservation (Fig. 3b; Yu et al., 2008, 2010, 2013) during the main purported geologic carbon pulses. Indeed, the temporal coincidence of the ^{14}C anomalies with stadial/interstadial climate change, deglacial ocean heat uptake (Poggemann et al., 2018), and circulation change (e.g., McManus et al., 2004; Rafter et al., 2022) may point to a climatic or environmental trigger of carbon release, rather than a being a purely volcanogenic phenomenon.

However, why would severe ^{14}C anomalies persist for millennia in the ETNP upper ocean water column if ocean circulation and air/sea gas exchange act to rapidly dissipate the anomalous carbon globally (Hain et al., 2011)? We propose two alternative resolutions that we cannot distinguish based on our current model and existing data: Either the anomalies are localized and reflect geologic carbon diffusion out of the underlying sediment stack rather than bottom water $\Delta^{14}C$, or the anomalies are regional and reflect the accumulation of geologic carbon in the ETNP shadow zone of ocean circulation with a sharp and persistent chemical gradient to the open ocean mid-depth Pacific.

If the anomalies are localized, we might expect each anomalous record to differ in magnitude and timing. Finding individual mid-depth sites in the ETNP where ^{14}C anomalies are missing (e.g., Bova et al., 2018; Chen et al., 2020) alongside records with ^{14}C anomalies that are only broadly similar, would tend to support the localized explanation. Conversely, if geologic carbon were added to a dynamically isolated region, such as the upper ocean ETNP (Margolskee et al., 2019), then seawater $\Delta^{14}C$ might diverge substantially from the $\Delta^{14}C$ of the open Pacific and atmosphere. However, that regional signal would still need to be shared by all radiocarbon records in the hydrodynamic region (cf. Chen et al., 2020). If the anomalies did reflect the restricted regional ocean circulation of the ETNP, it would seem plausible that the carbon release mechanism also operated in regions outside the ETNP but without producing characteristic seawater $\Delta^{14}C$ anomalies.

5 Conclusion

We document a set of carbon cycle model scenarios since the LGM that include substantial (800-2400 PgC) release of geologic carbon that appear broadly consistent with reconstructed atmospheric CO_2 rise, $\Delta^{14}C$ decline, and deep-sea $CaCO_3$ burial patterns. In all simulations, geologic carbon release is primarily bicarbonate ion, with minimal effect on simulated ocean pH and atmospheric CO_2. That is, the global carbon cycle is effectively blind to geologic carbon release if neutralized by an equivalent release of alkalinity (ALK-to-DIC ratio near 1). Hence, reconstructed CO_2 change does not require geologic carbon release nor constrain how much bicarbonate may have been released into the environment. One key outcome of our study is that large-scale geologic bicarbonate release since the LGM is possible.

Geologic carbon release dilutes the planetary inventory of cosmogenic radiocarbon (^{14}C), with 2400 Pg of ^{14}C-free carbon release reducing the average $\Delta^{14}C$ of environmental carbon by about ~50‰. Therefore, the planetary ^{14}C budget can be used to rule out the most extreme scenarios for geologic carbon release, offering an upper-bound constraint for carbon transfers from geologic and terrestrial carbon reservoirs to the ocean/atmosphere carbon cycle. That is, our model scenarios are designed to explore the limit of what appears to be possible in the context of global constraints from CO_2 and ^{14}C reconstructions. We find that bicarbonate release was likely limited to less than 1000 PgC. When considering uncertainty in the history of cosmogenic ^{14}C production, the limit for bicarbonate release may be as high as 2400 PgC.

The spatial cluster of severe negative deglacial $\Delta^{14}C$ anomalies in the upper water column of the ETNP may be evidence for geologic carbon release associated with the seafloor spreading center defining the East Pacific Rise (Fig. 1; (Lindsay et al., 2015; Marchitto et al., 2007; Rafter et al., 2018, 2019; Stott et al., 2009). Confirming or rejecting this hypothesis would have several implications: Without large-scale carbon release, we lack an adequate explanation for the ETNP $\Delta^{14}C$ anomalies, suggesting an open gap in our understanding of the ^{14}C-proxy system used to reconstruct ocean circulation changes in response to deglacial climate change. Alternatively, with large pulses of geologic carbon release in the ETNP, we lack an adequate explanation for how bicarbonate is derived from geologic carbon sources during the deglaciation, suggesting a gap in our understanding of glacial/interglacial changes in seafloor spreading and its role in the global carbon cycle. Further, if 1000 PgC or more of bicarbonate were released without causing ocean acidification or substantial CO_2 effects, the ETNP radiocarbon anomalies may hold lessons for mitigating and neutralizing anthropogenic carbon emissions via artificial Ocean Alkalinity Enhancement deployments.

Acknowledgments

This research was funded by the National Science Foundation (Collaborative Research Grants OCE-2032340 to MPH and OCE-2032340 to PAR).

Open Research

Detailed model description and configuration are available in the Supporting Information. The plotting code and simulation results are found on GitHub (https://github.com/RyanAGreen/Deglacial-Neutralized-Carbon-14C) and Zenodo (https://zenodo.org/badge/latestdoi/627637425).

References:

Adams, J. M., Faure, H., Faure-Denard, L., McGlade, J. M., & Woodward, F. I. (1990). Increases in terrestrial carbon storage from the Last Glacial Maximum to the present. *Nature*, *348*(6303), 711–714. https://doi.org/10.1038/348711a0

Allen, K. A., Sikes, E. L., Anderson, R. F., & Rosenthal, Y. (2020). Rapid Loss of CO2 From the South Pacific Ocean During the Last Glacial Termination. *Paleoceanography and Paleoclimatology*, *35*(2), e2019PA003766. https://doi.org/10.1029/2019PA003766

Allen, K. A., Sikes, E. L., Hönisch, B., Elmore, A. C., Guilderson, T. P., Rosenthal, Y., & Anderson, R. F. (2015). Southwest Pacific deep water carbonate chemistry linked to high southern latitude climate and atmospheric CO2 during the Last Glacial Termination. *Quaternary Science Reviews*, *122*, 180–191. https://doi.org/10.1016/j.quascirev.2015.05.007

Behling, H. (2002). Carbon storage increases by major forest ecosystems in tropical South America since the Last Glacial Maximum and the early Holocene. *Global and Planetary Change*, *33*(1), 107–116. https://doi.org/10.1016/S0921-8181(02)00065-6

Bereiter, B., Eggleston, S., Schmitt, J., Nehrbass-Ahles, C., Stocker, T. F., Fischer, H., Kipfstuhl, S., & Chappellaz, J. (2015). Revision of the EPICA Dome C CO2 record from 800 to 600 kyr before present. *Geophysical Research Letters*, *42*(2), 542–549. https://doi.org/10.1002/2014GL061957

Bova, S. C., Herbert, T. D., & Altabet, M. A. (2018). Ventilation of Northern and Southern Sources of Aged Carbon in the Eastern Equatorial Pacific During the Younger Dryas Rise in Atmospheric CO2. *Paleoceanography and Paleoclimatology*, *33*(11), 1151–1168. https://doi.org/10.1029/2018PA003386

Broecker, W. (2009). The Mysterious ^{14}C Decline. *Radiocarbon*, *51*(1), 109–119. https://doi.org/10.1017/S0033822200033737

Broecker, W., & Barker, S. (2007). A 190‰ drop in atmosphere's Δ14C during the "Mystery Interval" (17.5 to 14.5 kyr). *Earth and Planetary Science Letters*, *256*(1–2), 90–99. https://doi.org/10.1016/j.epsl.2007.01.015

Cartapanis, O., Galbraith, E. D., Bianchi, D., & Jaccard, S. L. (2018). Carbon burial in deep-sea sediment and implications for oceanic inventories of carbon and alkalinity over the last glacial cycle. *Climate of the Past*, *14*(11), 1819–1850. https://doi.org/10.5194/cp-14-1819-2018

Chen, T., Robinson, L. F., Burke, A., Claxton, L., Hain, M. P., Li, T., Rae, J. W. B., Stewart, J., Knowles, T. D. J., Fornari, D. J., & Harpp, K. S. (2020). Persistently well-ventilated intermediate-depth ocean through the last deglaciation. *Nature Geoscience*, *13*(11), Article 11. https://doi.org/10.1038/s41561-020-0638-6

Ciais, P., Tagliabue, A., Cuntz, M., Bopp, L., Scholze, M., Hoffmann, G., Lourantou, A., Harrison, S. P., Prentice, I. C., Kelley, D. I., Koven, C., & Piao, S. L. (2012). Large inert carbon pool in the terrestrial biosphere during the Last Glacial Maximum. *Nature Geoscience*, *5*(1), Article 1. https://doi.org/10.1038/ngeo1324

Crichton, K. A., Bouttes, N., Roche, D. M., Chappellaz, J., & Krinner, G. (2016). Permafrost carbon as a missing link to explain CO2 changes during the last deglaciation. *Nature Geoscience*, *9*(9), 683–686. https://doi.org/10.1038/ngeo2793

De Pol-Holz, R., Keigwin, L., Southon, J., Hebbeln, D., & Mohtadi, M. (2010). No signature of abyssal carbon in intermediate waters off Chile during deglaciation. *Nature Geoscience*, *3*(3), Article 3. https://doi.org/10.1038/ngeo745

Deutsch, C., Gruber, N., Key, R. M., Sarmiento, J. L., & Ganachaud, A. (2001). Denitrification and N2 fixation in the Pacific Ocean. *Global Biogeochemical Cycles*, *15*(2), 483–506. https://doi.org/10.1029/2000GB001291

Dinauer, A., Adolphi, F., & Joos, F. (2020). Mysteriously high $\Delta^{14}C$ of the glacial atmosphere: Influence of ^{14}C production and carbon cycle changes. *Climate of the Past*, *16*(4), 1159–1185. https://doi.org/10.5194/cp-16-1159-2020

Fine, R. A., Maillet, K. A., Sullivan, K. F., & Willey, D. (2001). Circulation and ventilation flux of the Pacific Ocean. *Journal of Geophysical Research: Oceans*, *106*(C10), 22159–22178. https://doi.org/10.1029/1999JC000184

Gehrie, E., Archer, D., Emerson, S., Stump, C., & Henning, C. (2006). Subsurface ocean argon disequilibrium reveals the equatorial Pacific shadow zone. *Geophysical Research Letters*, *33*(18). https://doi.org/10.1029/2006GL026935

Gruber, N., & Sarmiento, J. L. (1997). Global patterns of marine nitrogen fixation and denitrification. *Global Biogeochemical Cycles*, *11*(2), 235–266. https://doi.org/10.1029/97GB00077

Hain, M. P., Sigman, D. M., & Haug, G. H. (2010). Carbon dioxide effects of Antarctic stratification, North Atlantic Intermediate Water formation, and subantarctic nutrient drawdown during the last ice age: Diagnosis and synthesis in a geochemical box model. *Global Biogeochemical Cycles*, *24*(4), n/a-n/a. https://doi.org/10.1029/2010GB003790

Hain, M. P., Sigman, D. M., & Haug, G. H. (2011). Shortcomings of the isolated abyssal reservoir model for deglacial radiocarbon changes in the mid-depth Indo-Pacific Ocean. *Geophysical Research Letters*, *38*(4). https://doi.org/10.1029/2010GL046158

Hain, M. P., Sigman, D. M., & Haug, G. H. (2014). Distinct roles of the Southern Ocean and North Atlantic in the deglacial atmospheric radiocarbon decline. *Earth and Planetary Science Letters*, *394*, 198–208. https://doi.org/10.1016/j.epsl.2014.03.020

Hodell, D. A., Venz, K. A., Charles, C. D., & Ninnemann, U. S. (2003). Pleistocene vertical carbon isotope and carbonate gradients in the South Atlantic sector of the Southern Ocean. *Geochemistry, Geophysics, Geosystems*, *4*(1), 1–19. https://doi.org/10.1029/2002GC000367

Holzer, M., DeVries, T., & de Lavergne, C. (2021). Diffusion controls the ventilation of a Pacific Shadow Zone above abyssal overturning. *Nature Communications*, *12*(1), Article 1. https://doi.org/10.1038/s41467-021-24648-x

Huybers, P., & Langmuir, C. (2009). Feedback between deglaciation, volcanism, and atmospheric CO2. *Earth and Planetary Science Letters*, *286*(3), 479–491. https://doi.org/10.1016/j.epsl.2009.07.014

Ito, T., & Follows, M. J. (2005). Preformed phosphate, soft tissue pump and atmospheric CO2. *Journal of Marine Research*, *63*(4), 813–839. https://doi.org/10.1357/0022240054663231

Keir, R. S. (1988). On the Late Pleistocene ocean geochemistry and circulation. *Paleoceanography*, *3*(4), 413–445. https://doi.org/10.1029/PA003i004p00413

Köhler, P., Knorr, G., & Bard, E. (2014). Permafrost thawing as a possible source of abrupt carbon release at the onset of the Bølling/Allerød. *Nature Communications*, *5*(1), Article 1. https://doi.org/10.1038/ncomms6520

Lindgren, A., Hugelius, G., & Kuhry, P. (2018). Extensive loss of past permafrost carbon but a net accumulation into present-day soils. *Nature*, *560*(7717), Article 7717. https://doi.org/10.1038/s41586-018-0371-0

Lindsay, C. M., Lehman, S. J., Marchitto, T. M., Carriquiry, J. D., & Ortiz, J. D. (2016). New constraints on deglacial marine radiocarbon anomalies from a depth transect near Baja California. *Paleoceanography*, *31*(8), 1103–1116. https://doi.org/10.1002/2015PA002878

Lindsay, C. M., Lehman, S. J., Marchitto, T. M., & Ortiz, J. D. (2015). The surface expression of radiocarbon anomalies near Baja California during deglaciation. *Earth and Planetary Science Letters*, *422*, 67–74. https://doi.org/10.1016/j.epsl.2015.04.012

Marchitto, T. M., Lehman, S. J., Ortiz, J. D., Fluckiger, J., & van Geen, A. (2007). Marine Radiocarbon Evidence for the Mechanism of Deglacial Atmospheric CO_2 Rise. *Science*, *316*(5830), 1456–1459. https://doi.org/10.1126/science.1138679

Marchitto, T. M., Lynch-Stieglitz, J., & Hemming, S. R. (2005). Deep Pacific $CaCO_3$ compensation and glacial–interglacial atmospheric CO_2. *Earth and Planetary Science Letters*, *231*(3), 317–336. https://doi.org/10.1016/j.epsl.2004.12.024

Marcott, S. A., Bauska, T. K., Buizert, C., Steig, E. J., Rosen, J. L., Cuffey, K. M., Fudge, T. J., Severinghaus, J. P., Ahn, J., Kalk, M. L., McConnell, J. R., Sowers, T., Taylor, K. C., White, J. W. C., & Brook, E. J. (2014). Centennial-scale changes in the global carbon cycle during the last deglaciation. *Nature*, *514*(7524), Article 7524. https://doi.org/10.1038/nature13799

Margolskee, A., Frenzel, H., Emerson, S., & Deutsch, C. (2019). Ventilation Pathways for the North Pacific Oxygen Deficient Zone. *Global Biogeochemical Cycles*, *33*(7), 875–890. https://doi.org/10.1029/2018GB006149

Marinov, I., Follows, M., Gnanadesikan, A., Sarmiento, J. L., & Slater, R. D. (2008a). How does ocean biology affect atmospheric pCO_2? Theory and models. *Journal of Geophysical Research: Oceans*, *113*(C7). https://doi.org/10.1029/2007JC004598

Marinov, I., Gnanadesikan, A., Sarmiento, J. L., Toggweiler, J. R., Follows, M., & Mignone, B. K. (2008b). Impact of oceanic circulation on biological carbon storage in the ocean and atmospheric pCO_2. *Global Biogeochemical Cycles*, *22*(3). https://doi.org/10.1029/2007GB002958

McManus, J. F., Francois, R., Gherardi, J.-M., Keigwin, L. D., & Brown-Leger, S. (2004). Collapse and rapid resumption of Atlantic meridional circulation linked to deglacial climate changes. *Nature*, *428*(6985), Article 6985. https://doi.org/10.1038/nature02494

Poggemann, D.-W., Nürnberg, D., Hathorne, E. C., Frank, M., Rath, W., Reißig, S., & Bahr, A. (2018). Deglacial Heat Uptake by the Southern Ocean and Rapid Northward Redistribution Via Antarctic Intermediate Water. *Paleoceanography and Paleoclimatology*, *33*(11), 1292–1305. https://doi.org/10.1029/2017PA003284

Pollack, H. N., Hurter, S. J., & Johnson, J. R. (1993). Heat flow from the Earth’s interior: Analysis of the global data set. *Reviews of Geophysics*, *31*(3), 267–280. https://doi.org/10.1029/93RG01249

Rafter, P. A., Carriquiry, J. D., Herguera, J., Hain, M. P., Solomon, E. A., & Southon, J. R. (2019). Anomalous > 2000-Year-Old Surface Ocean Radiocarbon Age as Evidence for Deglacial Geologic Carbon Release. *Geophysical Research Letters*, *46*(23), 13950–13960. https://doi.org/10.1029/2019GL085102

Rafter, P. A., Gray, W. R., Hines, S. K. V., Burke, A., Costa, K. M., Gottschalk, J., Hain, M. P., Rae, J. W. B., Southon, J. R., Walczak, M. H., Yu, J., Adkins, J. F., & DeVries, T. (2022). Global reorganization of deep-sea circulation and carbon storage after the last ice age. *Science Advances*, *8*(46), eabq5434. https://doi.org/10.1126/sciadv.abq5434

Rafter, P. A., Herguera, J.-C., & Southon, J. R. (2018). Extreme lowering of deglacial seawater radiocarbon recorded by both epifaunal and infaunal benthic foraminifera in a wood-dated sediment core. *Climate of the Past*, *14*(12), 1977–1989. https://doi.org/10.5194/cp-14-1977-2018

Reimer, P. J., Austin, W. E. N., Bard, E., Bayliss, A., Blackwell, P. G., Ramsey, C. B., Butzin, M., Cheng, H., Edwards, R. L., Friedrich, M., Grootes, P. M., Guilderson, T. P., Hajdas, I., Heaton, T. J., Hogg, A. G., Hughen, K. A., Kromer, B., Manning, S. W., Muscheler, R., … Talamo, S. (2020). The IntCal20 Northern Hemisphere Radiocarbon Age Calibration Curve (0–55 cal kBP). *Radiocarbon*, *62*(4), 725–757. https://doi.org/10.1017/RDC.2020.41

Reimer, P. J., Baillie, M. G. L., Bard, E., Bayliss, A., Beck, J. W., Blackwell, P. G., Ramsey, C. B., Buck, C. E., Burr, G. S., Edwards, R. L., Friedrich, M., Grootes, P. M., Guilderson, T. P., Hajdas, I., Heaton, T. J., Hogg, A. G., Hughen, K. A., Kaiser, K. F., Kromer, B., … Weyhenmeyer, C. E. (2009). IntCal09 and Marine09 Radiocarbon Age Calibration Curves, 0–50,000 Years cal BP. *Radiocarbon*, *51*(4), 1111–1150. https://doi.org/10.1017/S0033822200034202

Reimer, P. J., Bard, E., Bayliss, A., Beck, J. W., Blackwell, P. G., Ramsey, C. B., Buck, C. E., Cheng, H., Edwards, R. L., Friedrich, M., Grootes, P. M., Guilderson, T. P., Haflidason, H., Hajdas, I., Hatté, C., Heaton, T. J., Hoffmann, D. L., Hogg, A. G., Hughen, K. A., … Plicht, J. van der. (2013). IntCal13 and Marine13 Radiocarbon Age Calibration Curves 0–50,000 Years cal BP. *Radiocarbon*, *55*(4), 1869–1887. https://doi.org/10.2458/azu_js_rc.55.16947

Ronge, T. A., Tiedemann, R., Lamy, F., Köhler, P., Alloway, B. V., De Pol-Holz, R., Pahnke, K., Southon, J., & Wacker, L. (2016). Radiocarbon constraints on the extent and evolution of the South Pacific glacial carbon pool. *Nature Communications*, *7*(1), 11487. https://doi.org/10.1038/ncomms11487

Rose, K. A., Sikes, E. L., Guilderson, T. P., Shane, P., Hill, T. M., Zahn, R., & Spero, H. J. (2010). Upper-ocean-to-atmosphere radiocarbon offsets imply fast deglacial carbon dioxide release. *Nature*, *466*(7310), Article 7310. https://doi.org/10.1038/nature09288

Roth, R., & Joos, F. (2012). Model limits on the role of volcanic carbon emissions in regulating glacial–interglacial CO2 variations. *Earth and Planetary Science Letters*, *329–330*, 141–149. https://doi.org/10.1016/j.epsl.2012.02.019

Roth, R., & Joos, F. (2013). A reconstruction of radiocarbon production and total solar irradiance from the Holocene ^{14}C and CO_2 records: Implications of data and model uncertainties. *Climate of the Past*, *9*(4), 1879–1909. https://doi.org/10.5194/cp-9-1879-2013

ScienceDirect Snapshot. (n.d.). Retrieved September 9, 2022, from https://www.sciencedirect.com/science/article/pii/S0277379113002400

Siani, G., Michel, E., De Pol-Holz, R., DeVries, T., Lamy, F., Carel, M., Isguder, G., Dewilde, F., & Lourantou, A. (2013). Carbon isotope records reveal precise timing of enhanced Southern Ocean upwelling during the last deglaciation. *Nature Communications*, *4*(1), Article 1. https://doi.org/10.1038/ncomms3758

Sigman, D. M., Fripiat, F., Studer, A. S., Kemeny, P. C., Martínez-García, A., Hain, M. P., Ai, X., Wang, X., Ren, H., & Haug, G. H. (2021). The Southern Ocean during the ice ages: A review of the Antarctic surface isolation hypothesis, with comparison to the North Pacific. *Quaternary Science Reviews*, *254*, 106732. https://doi.org/10.1016/j.quascirev.2020.106732

Sigman, D. M., Hain, M. P., & Haug, G. H. (2010). The polar ocean and glacial cycles in atmospheric CO 2 concentration. *Nature*, *466*(7302), 47–55. https://doi.org/10.1038/nature09149

Sigman, D. M., & Haug, G. H. (2003). *6.18 The Biological Pump in the Past*.

Skinner, L. C., & Bard, E. (2022). Radiocarbon as a Dating Tool and Tracer in Paleoceanography. *Reviews of Geophysics*, *60*(1), e2020RG000720. https://doi.org/10.1029/2020RG000720

Skinner, L. C., Fallon, S., Waelbroeck, C., Michel, E., & Barker, S. (2010). Ventilation of the Deep Southern Ocean and Deglacial CO2 Rise. *Science*, *328*(5982), 1147–1151. https://doi.org/10.1126/science.1183627

Stott, L. D., Harazin, K. M., & Krupinski, N. B. Q. (2019). Hydrothermal carbon release to the ocean and atmosphere from the eastern equatorial Pacific during the last glacial termination. *Environmental Research Letters*, *14*(2), 025007. https://doi.org/10.1088/1748-9326/aafe28

Stott, L., Southon, J., Timmermann, A., & Koutavas, A. (2009). Radiocarbon age anomaly at intermediate water depth in the Pacific Ocean during the last deglaciation. *Paleoceanography*, *24*(2), n/a-n/a. https://doi.org/10.1029/2008PA001690

Stott, L., & Timmermann, A. (2011). Hypothesized Link Between Glacial/Interglacial Atmospheric CO2 Cycles and Storage/Release of CO2-Rich Fluids From Deep-Sea Sediments. In H. Rashid, L. Polyak, & E. Mosley-Thompson (Eds.), *Geophysical Monograph Series* (Vol. 193, pp. 123–138). American Geophysical Union. https://doi.org/10.1029/2010GM001052

Stuiver, M., & Polach, H. A. (1977). Discussion Reporting of 14C Data. *Radiocarbon*, *19*(3), 355–363. https://doi.org/10.1017/S0033822200003672

Yu, J., Anderson, R. F., Jin, Z., Menviel, L., Zhang, F., Ryerson, F. J., & Rohling, E. J. (2014). Deep South Atlantic carbonate chemistry and increased interocean deep water exchange during last deglaciation. *Quaternary Science Reviews*, *90*, 80–89. https://doi.org/10.1016/j.quascirev.2014.02.018

Yu, J., Anderson, R. F., Jin, Z., Rae, J. W. B., Opdyke, B. N., & Eggins, S. M. (2013). Responses of the deep ocean carbonate system to carbon reorganization during the Last Glacial–interglacial cycle. *Quaternary Science Reviews*, *76*, 39–52. https://doi.org/10.1016/j.quascirev.2013.06.020

Yu, J., Broecker, W. S., Elderfield, H., Jin, Z., McManus, J., & Zhang, F. (2010). Loss of Carbon from the Deep Sea Since the Last Glacial Maximum. *Science*, *330*(6007), 1084–1087. https://doi.org/10.1126/science.1193221

Yu, J., Elderfield, H., & Piotrowski, A. M. (2008). Seawater carbonate ion-δ13C systematics and application to glacial–interglacial North Atlantic ocean circulation. *Earth and Planetary Science Letters*, *271*(1), 209–220. https://doi.org/10.1016/j.epsl.2008.04.010

Zhao, N., & Keigwin, L. D. (2018). An atmospheric chronology for the glacial-deglacial Eastern Equatorial Pacific. *Nature Communications*, *9*(1), Article 1. https://doi.org/10.1038/s41467-018-05574-x

References From the Supporting Information:

Bereiter, B., Eggleston, S., Schmitt, J., Nehrbass-Ahles, C., Stocker, T. F., Fischer, H., Kipfstuhl, S., & Chappellaz, J. (2015). Revision of the EPICA Dome C CO2 record from 800 to 600 kyr before present. *Geophysical Research Letters*, *42*(2), 542–549. https://doi.org/10.1002/2014GL061957

Dinauer, A., Adolphi, F., & Joos, F. (2020). Mysteriously high $\Delta^{14}C$ of the glacial atmosphere: Influence of ^{14}C production and carbon cycle changes. *Climate of the Past*, *16*(4), 1159–1185. https://doi.org/10.5194/cp-16-1159-2020

Galbraith, E. D., Kwon, E. Y., Bianchi, D., Hain, M. P., & Sarmiento, J. L. (2015). The impact of atmospheric pCO2 on carbon isotope ratios of the atmosphere and ocean. *Global Biogeochemical Cycles*, *29*(3), 307–324. https://doi.org/10.1002/2014GB004929

Hain, M. P., Sigman, D. M., & Haug, G. H. (2010). Carbon dioxide effects of Antarctic stratification, North Atlantic Intermediate Water formation, and subantarctic nutrient drawdown during the last ice age: Diagnosis and synthesis in a geochemical box model. *Global Biogeochemical Cycles*, *24*(4), n/a-n/a. https://doi.org/10.1029/2010GB003790

Hain, M. P., Sigman, D. M., & Haug, G. H. (2014). Distinct roles of the Southern Ocean and North Atlantic in the deglacial atmospheric radiocarbon decline. *Earth and Planetary Science Letters*, *394*, 198–208. https://doi.org/10.1016/j.epsl.2014.03.020

Kovaltsov, G. A., Mishev, A., & Usoskin, I. G. (2012). A new model of cosmogenic production of radiocarbon 14C in the atmosphere. *Earth and Planetary Science Letters*, *337–338*, 114–120. https://doi.org/10.1016/j.epsl.2012.05.036

Laj, C., Kissel, C., & Beer, J. (2004). High resolution global paleointensity stack since 75 kyr (GLOPIS-75) calibrated to absolute values. *Washington DC American Geophysical Union Geophysical Monograph Series*, *145*, 255–265. https://doi.org/10.1029/145GM19

Mackensen, A., & Schmiedl, G. (2019). Stable carbon isotopes in paleoceanography: Atmosphere, oceans, and sediments. *Earth-Science Reviews*, *197*, 102893. https://doi.org/10.1016/j.earscirev.2019.102893

Reimer, P. J., Austin, W. E. N., Bard, E., Bayliss, A., Blackwell, P. G., Ramsey, C. B., Butzin, M., Cheng, H., Edwards, R. L., Friedrich, M., Grootes, P. M., Guilderson, T. P., Hajdas, I., Heaton, T. J., Hogg, A. G., Hughen, K. A., Kromer, B., Manning, S. W., Muscheler, R., … Talamo, S. (2020). The IntCal20 Northern Hemisphere Radiocarbon Age Calibration Curve (0–55 cal kBP). *Radiocarbon*, *62*(4), 725–757. https://doi.org/10.1017/RDC.2020.41

Reimer, P. J., Bard, E., Bayliss, A., Beck, J. W., Blackwell, P. G., Ramsey, C. B., Buck, C. E., Cheng, H., Edwards, R. L., Friedrich, M., Grootes, P. M., Guilderson, T. P., Haflidason, H., Hajdas, I., Hatté, C., Heaton, T. J., Hoffmann, D. L., Hogg, A. G., Hughen, K. A., … Plicht, J. van der. (2013). IntCal13 and Marine13 Radiocarbon Age Calibration Curves 0–50,000 Years cal BP. *Radiocarbon*, *55*(4), 1869–1887. https://doi.org/10.2458/azu_js_rc.55.16947

Roth, R., & Joos, F. (2013). A reconstruction of radiocarbon production and total solar irradiance from the Holocene ^{14}C and CO_2 records: Implications of data and model uncertainties. *Climate of the Past*, *9*(4), 1879–1909. https://doi.org/10.5194/cp-9-1879-2013

Sigman, D. M., Fripiat, F., Studer, A. S., Kemeny, P. C., Martínez-García, A., Hain, M. P., Ai, X., Wang, X., Ren, H., & Haug, G. H. (2020). The Southern Ocean during the ice ages: A review of the Antarctic surface isolation hypothesis, with comparison to the North Pacific. *Quaternary Science Reviews*, 106732. https://doi.org/10.1016/j.quascirev.2020.106732

Skinner, L. C., & Bard, E. (2022). Radiocarbon as a Dating Tool and Tracer in Paleoceanography. *Reviews of Geophysics*, *60*(1), e2020RG000720. https://doi.org/10.1029/2020RG000720

Stott, L., Davy, B., Shao, J., Coffin, R., Pecher, I., Neil, H., Rose, P., & Bialas, J. (2019). CO2 Release From Pockmarks on the Chatham Rise-Bounty Trough at the Glacial Termination. *Paleoceanography and Paleoclimatology*, *34*(11), 1726–1743. https://doi.org/10.1029/2019PA003674